AD-A116 750 CALIFORNIA UNIV SANTA BARBARA QUANTUM INST F/G 11/6
ALUMINUM CORROSION: CORRELATIONS OF CORROSION RATE WITH SURFACE--ETC(U)
JUN 82 Q G SHU, P J LOVE, A BAYMAN N00014-78-C-0011
UNCLASSIFIED TR-10 NL

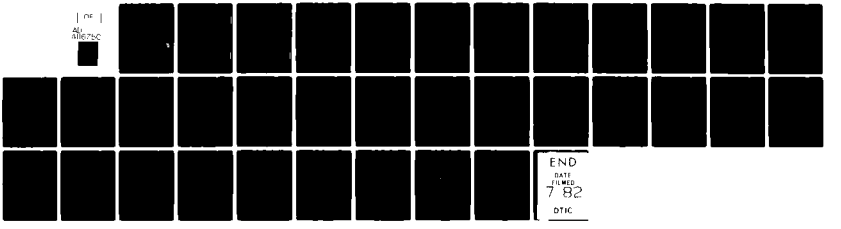

END
DATE FILMED
7 82
DTIC

12

OFFICE OF NAVAL RESEARCH
Contract N0014-78-C-0011
Task No. NR065-673
Technical Report 10

Aluminum Corrosion: Correlations of Corrosion Rate with Surface Coverage and Tunneling Spectra of Organic Inhibitors

by

Q. Q. Shu, P. J. Love, A. Bayman and P. K. Hansma

Prepared for Publication

in

Applications of Surface Science

University of California, Santa Barbara
Department of Physics
Quantum Institute

June 1982

SECURITY CLASSIFICATION OF THIS PAGE *(When Data Entered)*

REPORT DOCUMENTATION PAGE		READ INSTRUCTIONS BEFORE COMPLETING FORM
1. REPORT NUMBER	2. GOVT ACCESSION NO. AD-A116 750	3. RECIPIENT'S CATALOG NUMBER
4. TITLE *(and Subtitle)* Aluminum Corrosion: Correlations of Corrosion Rate with Surface Coverage and Tunneling Spectra of Organic Inhibitors		5. TYPE OF REPORT & PERIOD COVERED Technical
		6. PERFORMING ORG. REPORT NUMBER
7. AUTHOR(s) Q. Q. Shu, P. J. Love, A. Bayman and P. K. Hansma		8. CONTRACT OR GRANT NUMBER(s) N00014-78-C-0011
9. PERFORMING ORGANIZATION NAME AND ADDRESS Department of Physics, Quantum Institute University of California Santa Barbara, CA 93106		10. PROGRAM ELEMENT, PROJECT, TASK AREA & WORK UNIT NUMBERS NR056-6731
11. CONTROLLING OFFICE NAME AND ADDRESS Office of Naval Research Department of the Navy Arlington, VA 22217		12. REPORT DATE June, 1982
		13. NUMBER OF PAGES 33
14. MONITORING AGENCY NAME & ADDRESS*(if different from Controlling Office)*		15. SECURITY CLASS. *(of this report)* Unclassified
		15a. DECLASSIFICATION/DOWNGRADING SCHEDULE

16. DISTRIBUTION STATEMENT *(of this Report)*

Approved for public release and sale; distribution unlimited.

17. DISTRIBUTION STATEMENT *(of the abstract entered in Block 20, if different from Report)*

18. SUPPLEMENTARY NOTES

19. KEY WORDS *(Continue on reverse side if necessary and identify by block number)*

Corrosion, Organic Inhibitors, Tunneling Spectroscopy

20. ABSTRACT *(Continue on reverse side if necessary and identify by block number)*

Thin films of evaporated aluminum form a convenient model system for studying corrosion and corrosion inhibition on aluminum because 1) corrosion can be conveniently and continuously monitored by both electrical resistance measurements and optical transmission 2) surface coverage of inhibitor species can be measured by other radiotracer techniques or tunneling spectroscopy and 3) the nature of surface adsorbed species can be

(over)

DD FORM 1 JAN 73 1473 EDITION OF 1 NOV 65 IS OBSOLETE
S/N 0102-LF-014-6601

SECURITY CLASSIFICATION OF THIS PAGE *(When Data Entered)*

determined with tunneling spectroscopy. The corrosion rate for these films is of order 20 μm/yr in pure water at flow rates of order 20 cm/sec. The corrosion is inhibited by roughly one order of magnitude by monolayer surface coverages of the surface species that result when acetic acid, benzoic acid, cupferron or ethylene glycol are added to the water. At surface coverages of order 1/100 of a monolayer, the corrosion rate is increased by roughly an order of magnitude for the first three additivies but not for ethylene glycol. From the previous studies of tunneling spectra, it is clear that the acetic and benzoic acids lose a proton to become benzoate and acetate ions on the surface. The ethylene glycol loses the protons from both of its OH groups during bonding. The spectrum of the adsorbed cupferron species is presented but not analyzed.

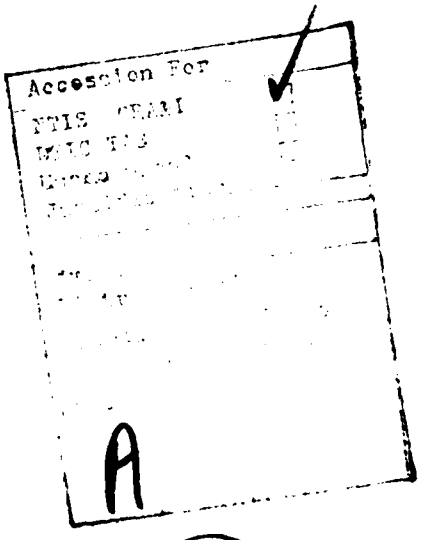

Aluminum Corrosion: Correlations of Corrosion Rate with Surface Coverage and Tunneling Spectra of Organic Inhibitors

Q. Q. Shu, P. J. Love, A. Bayman and P. K. Hansma

Department of Physics
University of California
Santa Barbara, CA 93106

Abstract

Thin films of evaporated aluminum form a convenient model system for studying corrosion and corrosion inhibition on aluminum because 1) corrosion can be conveniently and continuously monitored by both electrical resistance measurements and optical transmission, 2) surface coverage of inhibitor species can be measured by either radiotracer techniques or tunneling spectroscopy and 3) the nature of surface adsorbed species can be determined with tunneling spectroscopy. The corrosion rate for these films is of order 20 μm/yr in pure water at flow rates of order 20 cm/sec. The corrosion is inhibited by roughly one order of magnitude by monolayer surface coverages of the surface species that result when acetic acid, benzoic acid, cupferron or ethylene glycol are added to the water. At surface coverages of order 1/100 of a monolayer, the corrosion rate is increased by roughly an order of magnitude for the first three additives but not for ethylene glycol. From the previous studies of tunneling spectra, it is clear that the acetic and benzoic acids lose a proton to become benzoate and acetate ions on the surface. The ethylene glycol loses the protons from both of its OH groups during bonding. The spectrum of the adsorbed cupferron species is presented but not analyzed.

Introduction

Numerous authors have stressed the role played by surface coverage in determining corrosion inhibition by organic inhibitors. Surface coverage has been measured by a variety of techniques [1] including solution depletion methods[2,3], radiotracer techniques[4,5], infrared studies[6,7], changes in the capacitance of the electrical double layer[8,9], x-ray photoelectron spectroscopy [10] and Auger analysis [11]. Many of these studies provide adsorption isotherms: plots of surface coverage versus solution concentration (at fixed temperature).

Similarly, the effect of solution concentration on corrosion rate has been measured by many authors [12,13] in many ways including weight loss [14], resistance measurements [15] and a variety of electrochemical techniques [16].

Clearly it would be useful to know exactly what surface species were present on a surface and what their concentrations were during a corrosion rate measurement. This goal can be approached, if not reached, by choosing a special model system: thin films of pure aluminum. On this system tunneling spectroscopy can reveal the exact nature of the surface species, tunneling intensity measurements and radiotracer techniques can reveal the surface coverage, and simple electrical resistance or optical transmission measurements can give the corrosion rate.

The application of tunneling spectroscopy to corrosion was first made by Ellialtioglŭ, et al. [17] who studied corrosion by CCl_4. Here, we report results for acetic acid, benzoic acid, cupferron and ethylene glycol in water. Previous tunneling spectroscopy studies revealed that the two acids bond as symmetric, bidentate carboxylate anions [18]. Tunneling spectra

of the cupferron surface species are presented but not analyzed. In these three cases, saturation of corrosion inhibition with solution concentration was correlated with saturation of surface coverage. At surface coverages of order 0.01 monolayer, the first three compounds produced accelerated corrosion, as noted previously by other authors on other systems [19]. In the case of ethylene glycol, saturation of corrosion inhibition occurred at quite high solution concentrations and no accelerated corrosion was observed.

Apparatus

Evaporated aluminum films were corroded by fluids at a flow rate of 20 cm/sec in a flow cell. As shown in Fig. 1, the flow cell consisted of four basic parts: 1) two glass fluid reservoirs, one of which contained purified water, the other purified water plus an organic dopant, 2) an aluminum heat block which served as a heat sink, 3) a teflon block in which channels had been milled to allow the flow of fluid over films in contact with the channels and 4) glass slides on which the aluminum films were evaporated. The glass slides were compressed between the aluminum heat block and the teflon block to form a fluid-tight seal. A two-way teflon valve permitted flow of fluid from either fluid reservoir across the films with rapid switching between reservoirs. Teflon tubing conducted the fluids from each reservoir to the teflon block through a water-filled temperature reservoir which served as a heat exchanger between the fluids and the aluminum heat block.

The temperature reservoir, together with the aluminum heat block, served to minimize temperature gradients in the evaporated aluminum films and temperature differences between the sample fluids and the films. Near isothermal operation of the apparatus made it possible to make extremely sensitive resistance change measurements without interference from changes in film resistance caused by temperature fluctuations. Teflon construction was used throughout the apparatus to minimize the possibility of contamination of the sample fluids.

A detailed schematic of the Teflon block is shown in Fig. 2. Two shallow channels 0.13 mm in depth on one face of the teflon block provided fluid flow over the films in contact with the channels. These identical channels were 1.78 mm in width by 63.50 mm in length. The figure shows top, side and both end views of the block. Note that only one inlet tube fed both channels but that two outlet tubes were provided, one for each channel. The reasons for the use of two different fluid channels and the geometry described above will become clear in the following section where resistance change measurements will be described.

In our experiments, corrosion rates of evaporated aluminum films were determined by measuring electrical resistance and optical transmission of the corroded films.

The resistance measurement in the flow cell naturally includes the solution resistance. We measured the solution resistance separately in the second channel by means of the discontinuous strips shown in Fig. 2. This resistance is generally very large compared to the resistance of the film

($R_{solution}/R_{film} \simeq 100$). A Wheatstone bridge was used to cancel out the resistance of the solution. The circuit for the bridge is shown in Fig. 3. A lock-in amplifier was used as a synchronous detector to measure the signal voltage across the bridge. An A.C. bridge was used to help avoid polarization effects associated with the fluids in the channels.

Optical transmission was measured by mounting the slides between a He-Ne laser (6328 Å) and a photocell detector. A current-to-voltage converter was used to convert the output of the photocell directly into a voltage reading. The photocell exhibited linearity over a wide range in intensity of the transmitted light. Transmission was determined from the dimensionless ratio of transmitted intensity due to both film and slide to that due to the uncoated slide alone.

The apparatus used in radioactive labeling techniques [20] and inelastic electron tunneling technique [21-23] were described previously.

Sample Preparation

Aluminum strips of width 1.30 mm were evaporated onto glass slides at pressures of 2×10^{-5} torr. Film thickness was measured during the evaporation with a quartz crystal thickness monitor. Electrical connections were made to each end of the aluminum strip with indium solder (see Fig. 2). The slides were then mounted in the flow cell.

A Milli-Q (Millipore) water purification system was used to provide pure water for preparation of the sample solutions.

The unit delivered water at a resistivity of 15 MΩ - cm with final filtration through a 0.22 micron filter.

Tunneling junctions [21] were prepared by evaporating an aluminum strip (80 nm thick) onto a glass slide in high vacuum of order 10^{-6} torr. The aluminum strip was subsequently oxidized by venting the chamber to pure oxygen and then removing the slides from the chamber into air. This formed an insulating oxide layer roughly 20 Å thick[21].The oxide surface was doped by placing a drop of an aqueous solution of the compound of interest onto the junction area and spinning the excess off[22]. The junction was completed by evaporating a 2000 Å thick lead cross strip. The completed junctions were mounted on a probe with electrical contacts and immersed into liquid helium at 4.2 K where the current-voltage characteristics were studied.

Experimental Procedures

First, two independent measurements of the corrosion rate of evaporated aluminum films by distilled water alone were made by: 1) measurements of film resistance versus time (Ω/sec) inside the flow cell and 2) external measurements of optical transmission of the films versus time. These measurements were calibrated by measuring the resistance and optical transmission of evaporated aluminum films of known thickness as shown in Figs. 4 and 5. The thicknesses of the evaporated films were measured with a quartz crystal thickness monitor which was, in turn, calibrated with an optical interferometer.

The resultant corrosion rates were 24 ± 4 μm/yr by the resistance method and 19 ± 3 μm/yr by the optical transmission

method. This agreement gave us confidence in the results of the resistance method, which we used for almost all of the subsequent measurments since it was faster: instantaneous corrosion rates of order 20 μm/yr could be determined to 10% accuracy in measurement times of order 10 sec.

The resistance method was used to study the corrosion properties of four organic dopants at various solution concentrations. It was convenient to express the results in terms of a dimensionless relative corrosion inhibition parameter defined by the ratio of the slope of the resistance versus time of distilled water to that of distilled water plus dopant. In other words, the parameter is given by $(\Delta R/\Delta t)_w/(\Delta R/\Delta t)_s$ where w refers to distilled water and s refers to the organically doped solution. Values of the relative corrosion inhibition parameter greater than unity indicate that the dopant acts as a corrosion inhibitor while values less than unity indicate promotion of corrosion relative to distilled water. All of the corrosion measurements with the organic dopants were conducted on films of about the same thickness range of 29 nm to 25 nm (corresponding to a film resistance range of 250 Ω to 350 Ω). The reason for this restriction is to allow us more confidence in comparing the results of measurements on various samples. This range is also convenient: for thicker films the slope of resistance versus thickness is smaller and harder to measure, for thinner films the resistance can climb so fast that measurement time is limited.

The surface coverages of the four organic dopants at various solution concentrations were determined by two methods:

1) For acetic acid and benzoic acid, the surface concentration as a function of solution concentration on evaporated films of aluminum had previously been determined by radiotracer studies performed in our laboratory [20] and at the University of Pennsylvania [24].

2) For cuperferron it was determined by measuring the peak intensity in the inelastic electron tunneling spectra of junctions doped with a solution of the compound at various concentrations. As shown previously, the tunneling peak height is a monotonic function of surface coverage [20]. Unfortunately, it cannot be assumed to be linear but increases somewhat more rapidly than the surface coverage. For the case of benzoic acid, for example, the tunneling peak height was proportional to roughly the 4/3 power of surface concentration [20]. Nevertheless tunneling peak height gives a clear indication of the solution concentration that corresponds to a monolayer surface coverage. Of course, it has the important bonus that it gives a detailed vibrational spectra of the surface species. Thus, its exact chemical nature can, in principle at least, be determined.

Several experimental checks were performed in order to insure that the results of the corrosion measurements did not depend on the operating conditions. Two factors were considered which are worth mentioning here: 1) the influence of dissolved oxygen (or lack of it) in the distilled water used in the experiments and 2) the effect of changes in the measuring voltage applied across the sample films in the Wheatstone bridge arrangement. The influence of dissolved oxygen was checked by using distilled water from the Milli-Q system in one fluid reservoir of the flow cell and distilled water through which either dry nitrogen or oxygen gas was bubbled for at least one hour in the other.

For nitrogen, which presumably deoxygenated the water, the change in corrosion rate of the aluminum films upon switching between reservoirs was found to be negligibly small. For oxygen, the corrosion rate increased by about 30%.

The measured corrosion rate was found to be independent of measuring voltage throughout the range from one microvolt to 0.2 volt ($I_{film} \leq 1$ ma). Normal operating voltages were typically 0.15 volt.

Results

Fig. 6 shows plots of both relative corrosion inhibition parameter and surface concentration of acetic acid versus solution concentration. At concentrations greater than 2 mg/ml (3.3×10^{-2} M), the relative corrosion inhibition parameter of acetic acid approaches a plateau at a value of about seven. In this region, the surface concentration determined by radioactive labeling [23] is nearly fully saturated at about 5×10^{14} molecules/cm^2. This corresponds to a monolayer coverage. As the solution concentration drops, both the surface concentration and relative corrosion inhibition parameter decrease. At a concentration of 0.2 mg/ml (3.3×10^{-3} M) the relative corrosion inhibition parameter becomes unity indicating that the corrosion rate at this concentration is the same as that for distilled water. The surface concentration at this point has diminished by a factor of 20 from monolayer coverage. A furtner decrease in solution concentration below 0.2 mg/ml (3.3×10^{-3} M) results in promotion in the corrosion rate relative to distilled water. The maximum corrosion rate

occurs at about 5×10^{-3} mg/ml (8.3×10^{-5} M) at which point the relative corrosion inhibition parameter has dropped to about 0.15 (the corrosion rate is about 6.5 times larger than for distilled water). Below this concentration, the relative corrosion inhibition parameter again approaches unity as it must for low enough concentrations. Note that an extremely dilute solution (less than about 5×10^{-5} mg/ml (8.3×10^{-7} M) is required before the corrosion inhibition parameter becomes indistinguishable from unity.

Similar results have been obtained for benzoic acid (Fig. 7). Now monolayer coverages are approached at a much lower solution concentration: only 0.2 mg/ml (1.6×10^{-3} M). The relative corrosion inhibition parameter saturates at about 10. As for acetic acid, the relative corrosion inhibition decreases along with surface coverage (determined from radioactive labeling) [20] as the solution concentration decreases, but in this case the relative corrosion inhibition drops much faster with decreasing solution concentration than for acetic acid. At a concentration of about 0.04 mg/ml (3.3×10^{-4} M), the relative corrosion inhibition parameter becomes unity, and the surface concentration has decreased roughly by a factor of 5 from monolayer coverage. In contrast to the results for acetic acid, the slope of the corrosion curve in this region is apparently significantly greater than that of the surface concentration curve. Below the critical concentration of 0.04 mg/ml (3.3×10^{-4} M), the solution becomes more corrosive than distilled water with a maximum rate at a concentration near 5×10^{-3} mg/ml (4.1×10^{-5} M) (about a factor 6 greater than

distilled water). The relative corrosion inhibition parameter slowly increases toward unity again for concentrations less than 1×10^{-4} mg/ml (8.2×10^{-7} M).

Unfortunately, measurements of the surface concentration as a function of solution concentration for well defined samples are available for only a handful of compounds. Measuring them with the radioactive tracer technique used for acetic acid and benzoic acid depends on the availablity of radioactively labeled compounds. For the next two compounds we studied, cupferron and ethylene glycol, the radioactively labeled species were not conveniently available. Fortunately, there is an alternative. The peak heights in inelastic electron tunneling spectra provide a good indication of surface coverage [20]. Fig. 8 shows the corrosion inhibition versus solution concentration (previously shown in Fig. 7) along with the peak height of a particular peak in the inelastic electron tunneling spectra for benzoic acid. Note that here again the fall off in corrosion inhibition below monolayer surface coverage is clearly mirrored in the fall off in the inelastic tunneling peak. Comparison of Figs. 7 and 8 reveals that though the tunneling peak height is a good measure of surface concentration it drops faster than the surface concentration; in particular, the slope is about 4/3 times larger [20].

Cupferron has previously been shown to be an efficient organic inhibitor of aluminum corrosion[15,25]. As shown in Fig. 9, cupferron gives similar results to acetic and benzoic acids, but the range of concentrations over which it promotes corrosion is significantly smaller. The relative corrosion inhibition parameter drops more slowly with decreasing solution concentration and falls below unity only for concentrations less than about 8×10^{-3} mg/ml (4.8×10^{-5} M). The minimum value of the relative corrosion inhibition parameter near 3.5×10^{-3} mg/ml (2.1×10^{-5} M) is now approximately 0.37 which is roughly twice as large as those found for the acids. Since a direct measurement of the surface concentration in terms of radioactively labeling is not available for cupferron, the tunneling peak height was used as a measure of the surface concentration.

It should be noted that for cupferron the slope of tunneling peak height versus solution concentration is significantly less than that for benzoic acid (compare Figs 8 and 9). In general, this is in agreement with the slow decrease in the relative corrosion inhibition parameter though a meaningful comparison of the slopes of the two curves is impossible. The tunneling peak height now decreases by a factor 60 between its saturation value and the concentration at which the relative corrosion inhibition parameter becomes unity indicating the wide range over which cupferron acts as an effective corrosion inhibitor.

Fig. 10 shows tunneling spectra of cupferron, benzoic acid, acetic acid and distilled water liquid doped onto the oxide of an Al-oxide-Pb junction. Concentrations of all

three compounds correspond to monolayer coverage. The peaks at 415 cm^{-1} for cupferron and 686 cm^{-1} for benzoic acid were chosen for the peak height measurements because background peaks (i.e. peaks from distilled water alone) are minimal in these regions.

Results for ethylene glycol are shown in Fig. 11. This compound starts to inhibit corrosion only at relatively high concentrations (above 20 mg/ml, i.e. 0.32 M) reaching a maximum of relative corrosion inhibition parameter (about 10 times slower corrosion than distilled water) above about 800 mg/ml (12.9 M). Unlike the other organic compounds we studied, ethylene glycol exhibits no region in which corrosion is promoted. We were not able to obtain tunneling spectra for the compound from liquid solutions because of difficulty in removing excess liquid at high concentrations. Its spectrum from vapor doped samples was included and analyzed in a previous publication[26]. That analysis revealed that it ionically bound to the oxidized aluminum by losing the protons from both OH groups.

Finally, it is important to recall that all the above measurements were taken at a flow rate of 20 cm/sec in the flow cell. We noticed that at over flow rate range of 0 to 40 cm/sec the corrosion rate for distilled water increased more quickly with increasing flow rate than it did for benzoic acid in distilled water at a concentration 1 mg/ml (8.2×10^{-3} M). A detailed analysis of the flow rate dependence of the corrosion rate needs further study.

Discussion

The experimental results we have obtained show that a clear correlation exists between the surface coverage of organic dopant and the degree of corrosion inhibition. Saturation of the surface coverage always appears to occur at a solution concentration near that at which the corrosion inhibition saturates. As the solution concentration is decreased, both the relative corrosion inhibition and the surface coverage decrease - with comparable slopes. Acetic acid, benzoic acid and cupferron all inhibit corrosion for high enough surface coverages (typically greater than 1/20 of the monolayer coverage) but promote corrosion for lower surface coverages. In contrast, ethylene glycol always inhibits corrosion but does so only at quite high solution concentrations.

All the facts suggest that the primary mechanism for corrosion inhibition by these organic compounds is adsorption onto the film surface. Other workers have also found evidence that organic inhibitors act by surface adsorption [1,19]. Analysis of tunneling spectra measurements has revealed that both acetic and benzoic acids bond via the active COOH group as symmetric, bidentate carbonylate anions with the hydrocarbon groups oriented away from the surface [27]. Evidence also exists that aluminum oxide surfaces are normally occupied with OH groups due to the interaction of the surface with water molecules in a water-vapor rich or aqueous environment [28,29]. Thus, inhibition may occur not only by displacement of adsorbed water but by the formation of a hydrophobic network of hydrocarbon "tails" which extend into the solution and hinder the access of water molecules to the surface.

The fact that corrosion is actually promoted at low surface coverages suggests that this picture is not complete and that an additional mechanism(s) is also involved. A speculative explanation is that localized attack such as pitting occurred when inhibitors were present in small concentrations. At low surface coverage, i. e. at low solution concentration, some inhibitors accelerate corrosion since they reduce the effective anode area, and, if not completely effective, they lead to much higher anodic current density at any remaining anodic sites, thus localized attack happens [30]. It is not yet clear why some inhibitors just reduce the anodic reaction and others not, but one important fact is that no change in the nature of adsorbed species is seen in the tunneling spectra as the surface coverage is decreased.

Summary

The flow cell is an effective tool for the study of metal film corrosion by aqueous solutions. Resistance change measurements in a flow cell provided a simple yet sensitive means for measuring corrosion rates. Our measurements for the corrosion inhibition of acetic acid, benzoic acid and cupferron show that at low concentrations these compounds promote corrosion, but, at higher concentrations where the surface coverage exceeds a small fraction of a monolayer, they inhibit corrosion. Ethylene glycol does not promote corrosion and it is an inhibitor at high solution concentrations.

Acknowledgments

We thank Professor D. S. Cannell for support, the use of equipment and laboratory space for the flow cell measurements, Dr. E. McCafferty for a very useful discussion and the Office of Naval Research and the National Science Foundation (Grant Nos. DMR79-25430 and DMR79-10030) for partial support of this work.

References

[1] E. McCafferty, "Corrosion Control by Coatings", ed. H. Leidheiser, Jr. (Science Pr., Princeton, NJ, 1979).

[2] N. Hackerman and A. H. Roebuck, Ind. Eng. Chem. 46 (1954) 1481.

[3] A. C. Makrides and N. Hackerman, Ind. Eng. Chem. 47 (1955) 1773.

[4] J. O'M. Bockris and D. A. J. Swinkels, J. Electrochem. Soc. 111 (1964) 736.

[5] D. S. Newman, J. McCarthy and M. Heckaman, J. Electrochem. Soc. 118 (1971) 541.

[6] G. W. Poling, J. Electrochem. Soc. 114 (1967) 1209.

[7] S. Friberg and H. Muller, "5th Scandinavian Corrosion Congress", Copenhagen, 1968, Chapter 5.

[8] Z. Szklarska-Smialowska and B. Dus, Corrosion 23 (1967) 131.

[9] E. McCafferty and N. Hackerman, J. Electrochem. Soc. 119 (1972) 146.

[10] J. D. Wood, Corrosion 34 (1978) 70.

[11] J. B. Lumsden and Z. Szklarska-Smialowska, Corrosion 34 (1978) 169.

[12] S. M. Hassan, Y. A. Elawady, A. I. Ahmed and A. O. Baghlaf, Corrosion Sci. 19 (1979) 951.

[13] D. W. Samuels, K. Sotoudek and R. T. Foley, Corrosion 27 (1981) 92.

[14] F. A. Champion, "Corrosion Testing Procedures", 2nd ed. (Butler and Tanner, Ltd., London, 1964) p. 197.

[15] E. C. Winegartner, Corrosion 16 (1960) 99.

[16] M. G. Fontana and N. D. Greene, "Corrosion Engineering", (McGraw, Inc., NY, 1978) p. 342 and 439.

[17] R. M. Ellialtoglŭ, H. W. White, L. M. Godwin and T. Wolfram, J. Chem. Phys. 72 (1980) 5291.

[18] J. T. Hall and P. K. Hansma, Surf. Sci. 76 (1978) 61.

[19] G. Trabanelli and V. Carassiti, "Mechanism and Phenomenology of Organic Inhibitions", in Advances in Corrosion Science and Technology, Vol. 1 (Plenum Press, NY, 1970) p. 189.

[20] J. D. Langan and P. K. Hansma. Surf. Sci. 52 (1975) 215.

[21] P. K. Hansma, Physics Rep. 30 (1977) 162.

[22] P. K. Hansma and R. V. Coleman, Science 184 (1974) 1369.

[23] S. L. Cunningham, W. H. Weinberg and J. R. Hardy, "Inelastic Electron Tunneling Spectroscopy", ed T. Wolfram (Springer, Berlin, 1978).

[24] A. A. Cederberg, Surf. Sci. 103 (1981) 148.

[25] Von L. Horner and K. Mersel, Werkstoffe und Korrosion 29 (1978) 654.

[26] A. Bayman and P. K. Hansma, Nature 285 (1980) 97.

[27] P. K. Hansma, Physics Rep. 30 (1977) 172.

[28] P. K. Hansma, Physics Rep. 30 (1977) 193.

[29] B. F. Lewis, W. M. Bowser, J. L. Horn, Jr., T. Luu and W. H. Weinberg, J. Vac. Sci. Technol. 11 (1974) 262.

[30] H. P. Godard, W. B. Jepson, M. R. Bathwell and R. L. Kane, "The Corrosion of Light Metals", (John Wiley and Sons, Inc., NY, 1967) p. 192.

Figure Captions

Fig. 1. A sectional drawing of the flow cell. Fluids are driven by gravitational force to flow in the two channels. Flow rates can be adjusted by changing the height of the liquid levels. The two-way valve is used to switch fluids.

Fig. 2. A detail of the Teflon substrate block and the glass slide with evaporated aluminum film in Fig. 1. The channels are 1.78 mm wide and 0.13 mm deep. The initial thickness of the film is about 30 nm.

Fig. 3. The Wheatstone bridge for the flow cell includes two fixed resistors of resistance R = 10 KΩ. The contribution to current flow from the solution alone, $R_{solution}$, is nearly cancelled out by its inclusion in both sides of the bridge.

Fig. 4. Resistance versus thickness for the evaporated aluminum films used in the flow cell. For thickness measurements, a calibrated quartz crystal thin film monitor was used.

Fig. 5. Transmission versus thickness for the evaporated aluminum films used in the flow cell. The transmission was measured relative to the transmission of the glass slide alone with a He-Ne laser at 6328 Å.

Fig. 6. Surface concentration (left scale) and relative corrosion inhibition parameter (right scale) versus the solution concentration for acetic acid in water.

Fig. 7. Surface concentration (left scale) and relative corrosion inhibition parameter (right scale) versus the solution concentration for benzoic acid in water.

Fig. 8. Height of tunneling peak at 686 cm^{-1} (left scale) and relative corrosion inhibition parameter (right scale) versus solution concentration for benzoic acid in water.

Fig. 9. Height of tunneling peak at 415 cm^{-1} (left scale) and relative corrosion inhibition parameter (right scale) versus solution concentration for cupferron in water.

Fig. 10. Tunneling spectra of cupferron, benzoic acid, acetic acid and distilled water liquid doped onto the oxide of an Al-oxide-Pb junction. Analysis of these spectra reveals that the two acids bond as bidentate symmetric carboxylate ions.

Fig. 11. Relative corrosion inhibition parameter versus the solution concentration for ethylene glycol. Note the absence of any region of increased corrosion (the relative corrosion inhibition < 1) in contrast to the results for cupferron, acetic acid and benzoic acid.

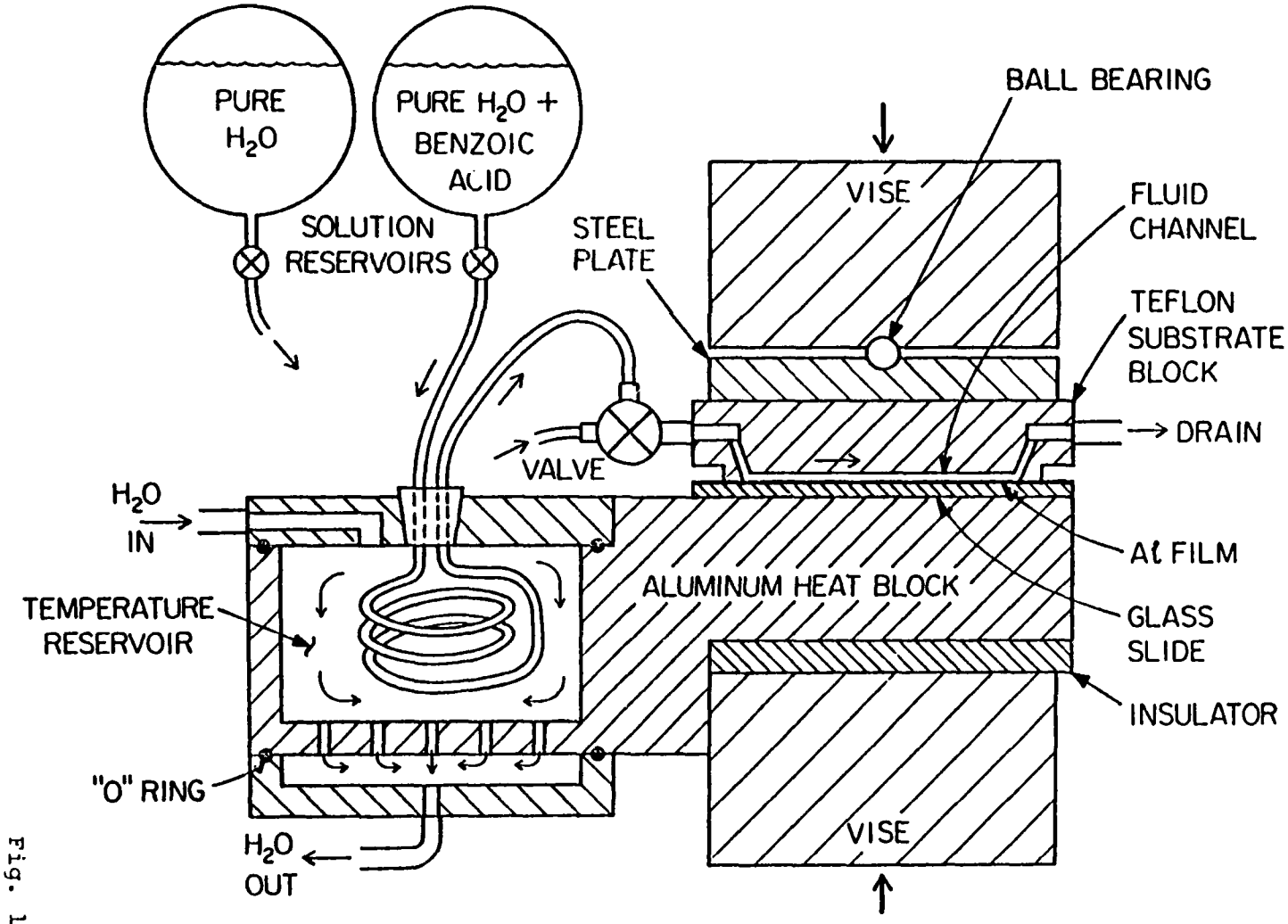

Shu, Love, Bayman & Hansma

Fig. 1

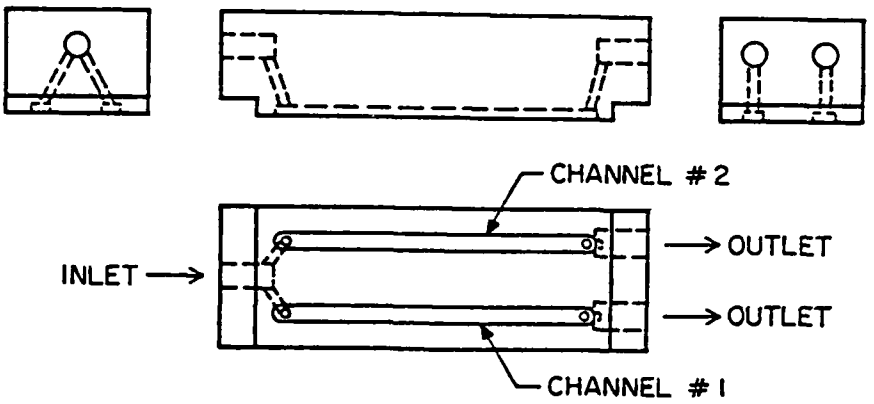

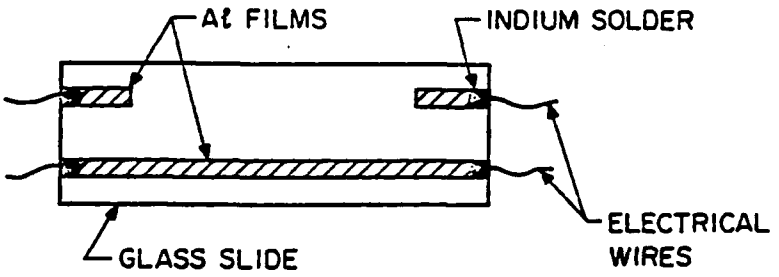

Fig. 2

Shu, Love,
Bayman & Hansma

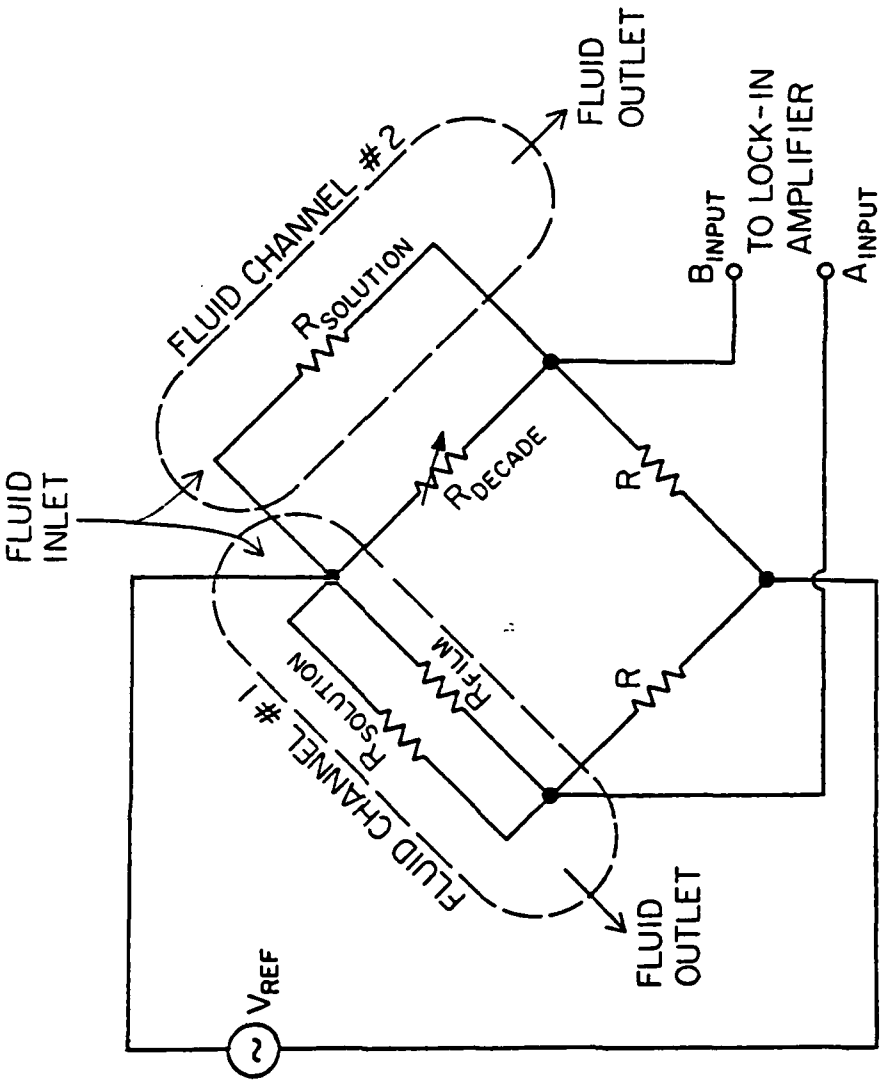

Fig. 3

Shu, Love,
Bayman & Hansma

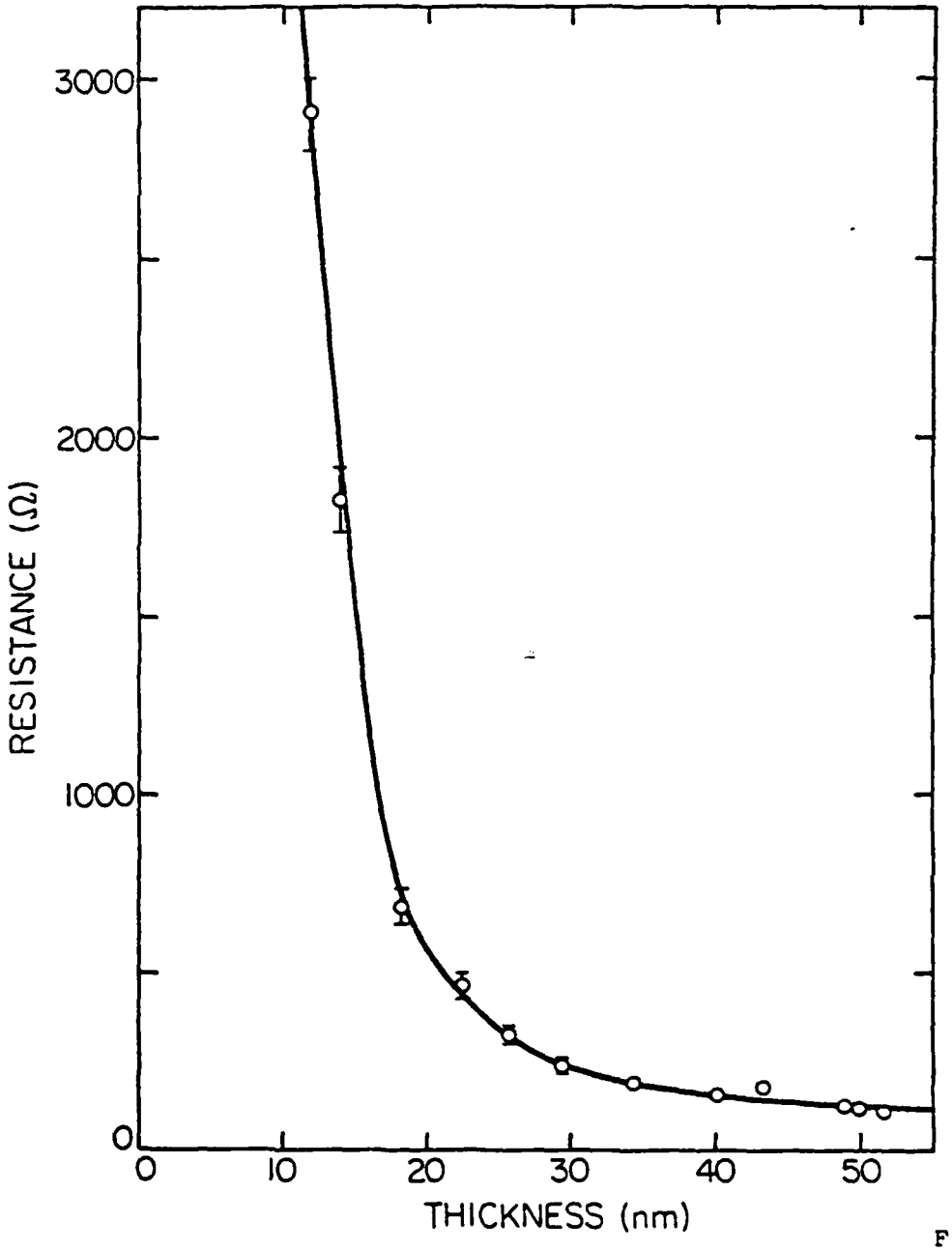

Fig. 4

Shu, Love,
Bayman & Hansma

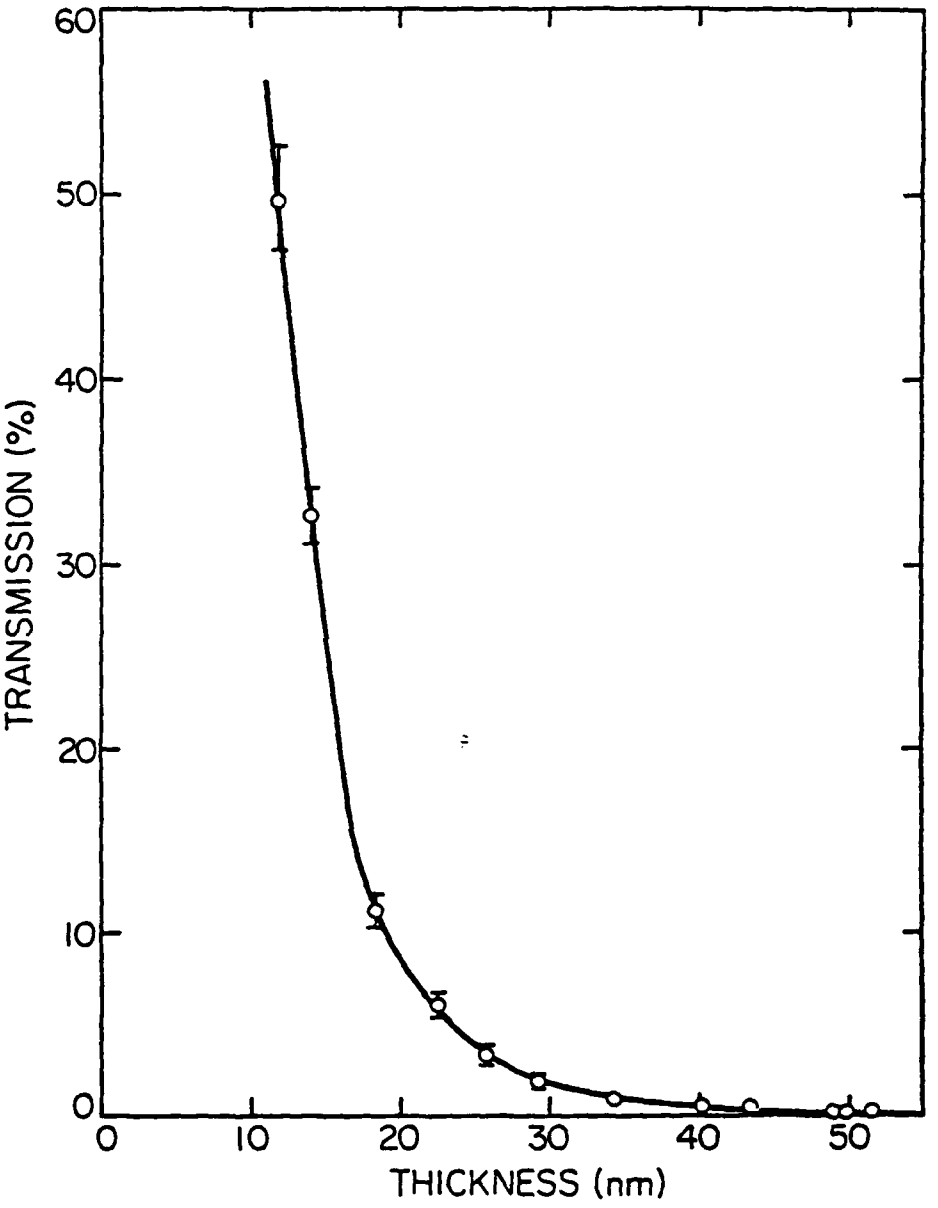

Fig. 5

Shu, Love,
Bayman & Hansma

Fig. 6

Shu, Love,
Bayman & Hansma

Fig. 7

Shu, Love,
Bayman & Hansma

Fig. 8

Shu, Love
Bayman & Hansma

Fig. 9

Shu, Love,
Bayman & Hansma

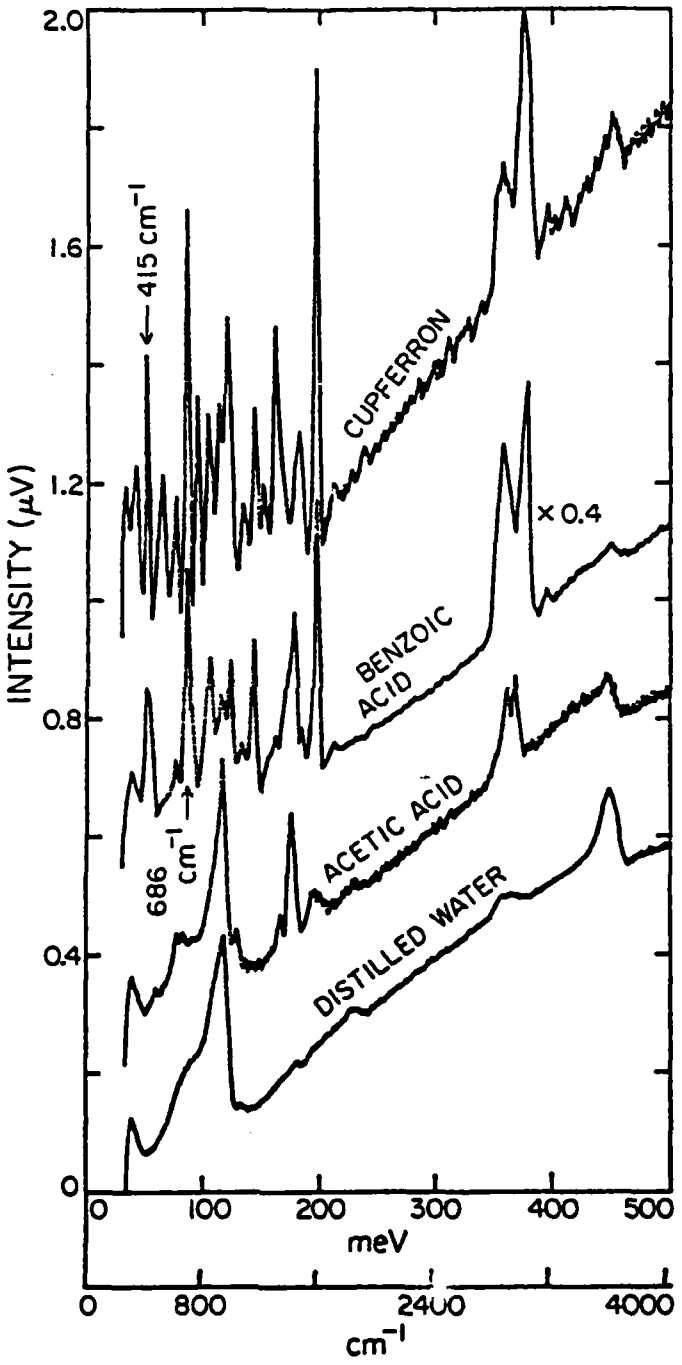

Fig. 10

Shu, Love,
Bayman & Hansma

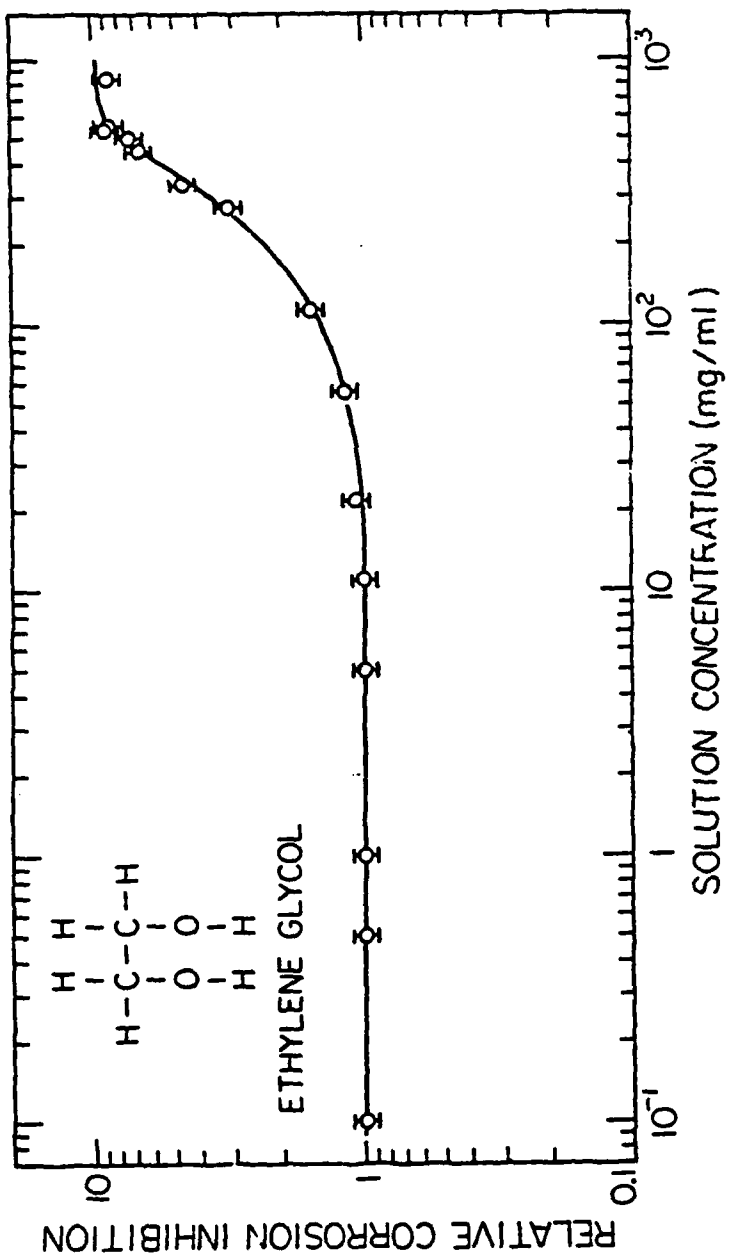

Fig. 11

Shu, Love,
Bayman & Hansma


DATE
ILME
8